Benzo[1,2-b:4,5-b']difuran-Based Donor-Acceptor Copolymers for Polymer Solar Cells

ARTICLE *in* MACROMOLECULES · SEPTEMBER 2012

Impact Factor: 5.8 · DOI: 10.1021/ma301053q

Macromolecules

Article

pubs.acs.org/Macromolecules

Benzo[1,2-*b*:4,5-*b*′]difuran-Based Donor−Acceptor Copolymers for Polymer Solar Cells

Bo Liu,[†,‡] Xuewen Chen,[†] Yingping Zou,*[,†] Lu Xiao,[†] Xinjun Xu,[§] Yuehui He,*[,‡] Lidong Li,[§] and Yongfang Li*[,⊥]

[†]College of Chemistry and Chemical Engineering, Central South University, Changsha 410083, China

[‡]State key Laboratory for Powder Metallurgy, Central South University, Changsha 410083, China

[§]School of Materials Science and Engineering, University of Science and Technology Beijing, Beijing 100083, China

[⊥]Beijing National Laboratory for Molecular Sciences, Institute of Chemistry, Chinese Academy of Sciences, Beijing 100190, China

Supporting Information

ABSTRACT: Three new benzo[1,2-*b*:4,5-*b*′]difuran-based donor−acceptor conjugated polymers, namely poly{4,8-bis(2′-ethylhexyloxy)benzo[1,2-*b*;3,4-*b*′]difuran-*alt*-5,5-(4′,7′-di-2-thienyl-5′,6′-dioctyloxy-2′,1′,3′-benzothiadiazole)}(**PBDFDODTBT**), poly{4,8-bis(2′-ethylhexyloxy)benzo-[1,2-*b*;3,4-*b*′]difuran-*alt*-5,5-(4′,7′-di-2-thienyl-2-octyl-2′,1′,3′-benzotriazole)}-(**PBDFDTBTz**), poly{4,8-bis(2′- ethylhexyloxy)benzo[1,2-*b*;3,4-*b*′]difuran-*alt*-5,5-(4′,7′-di-2-thienyl-5′,6′-dioctyloxy-benzo[*c*][1,2,5]oxadiazole)}-(**PBDFDTBO**), were synthesized by Stille coupling polymerization reactions. All of the polymers were found to be soluble in common organic solvents such as chloroform, tetrahydrofuran and chlorobenzene with excellent film forming properties. Their structures were verified by ^{1}H NMR and elemental analysis, the molecular weights were determined by gel permeation chromatography (GPC) and the thermal properties were investigated by thermogravimetric analysis (TGA) and differential scanning calorimetry (DSC). The polymer films exhibited broad absorption bands. The hole mobility of **PBDFDODTBT**:$PC_{71}BM$ (1:2, *w*/*w*) blend reached up to 6.7×10^{-2} $cm^2 \cdot V^{-1} \cdot s^{-1}$ by the space-charge-limited current (SCLC) method. Preliminary photovoltaic cells based on the device structure of ITO/PEDOT:PSS/**PBDFDODTBT**:$PC_{71}BM$(1:2, w/w)/Ca/Al showed an open-circuit voltage of 0.69 V, a power conversion efficiency of 4.5% and a short circuit current of 9.87 $mA \cdot cm^{-2}$.

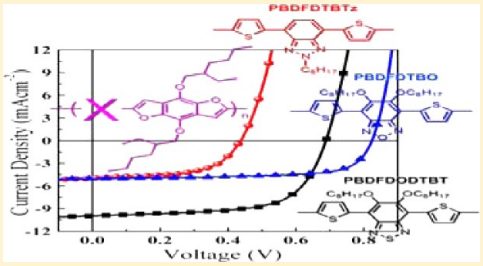

INTRODUCTION

Polymer solar cells (PSCs) have received broad attentions in both academia and industry in recent years, because of their some advantages of lightweight, flexibility, and low-cost.[1−5] Bulk heterojunction (BHJ) PSCs are composed of a photoactive blend layer of a conjugated polymer donor and a soluble fullerene derivative acceptor sandwiched between an indium−tin oxide (ITO) positive electrode and a low work function metal negative electrode.[6−8] Intensive researches on the molecular design and device optimization have led to a rapid development in the field of PSCs over the past decade.[9−12] During this process, the progresses are closely related to the new conjugated polymers. However, at this time, power conversion efficiency (PCE) and stability still need to be improved for commercial applications.[13] As well-known, the PCE is proportional to the open circuit voltage (V_{oc}), short circuit current (J_{sc}) and fill factor (FF) of the PSCs. Therefore, an ideal polymeric donor material should possess broad absorption spectra to harvest more sunlight for higher J_{sc}, deep HOMO level to maximize V_{oc} while keeping proper LUMO level for well charge separation with decreased energy loss, and higher hole mobility for higher J_{sc} and FF. Besides above parameters, molecular weight and nanoscale morphology are also needed to be optimized for higher PCEs.

Donor−acceptor (D-A) alternating copolymerization is a very effective strategy.[14] Recently, PCEs higher than 8% for D−A type polymers have been obtained.[15] Benzo[1,2-*b*:4,5-*b*′]dithiophene (BDT) as a most successful electron-donor unit has stimulated much interest because some BDT-based D−A copolymers with different acceptor moieties demonstrated high photovoltaic properties by structure modifications and device optimizations.[16] For example, Wu et al. improved the PCE of the PSC based on a low bandgap polymer PTB7, a copolymer of BDT and thieno[3,4-*b*]thiophene unit, up to 8.37% by using a thin layer of alcohol/water-soluble polymer as the cathode interlayer.[15] The advantages of BDT units include its planar conjugated structure, regioregularity, easy modification, and purification of BDT monomers; furthermore, some BDT-based polymers also show high hole mobility.

In addition to the application of these existing donors such as cyclopentadithiophene, dithienosilole, dithienopyrrole *etc*, it

Received: May 23, 2012
Revised: August 14, 2012
Published: August 27, 2012

   dx.doi.org/10.1021/ma301053q | *Macromolecules* 2012, 45, 6898−6905

Scheme 1. Synthesis and Structures of the Polymers PBDFDODTBT, PBDFDTBTz, and PBDFDTBO

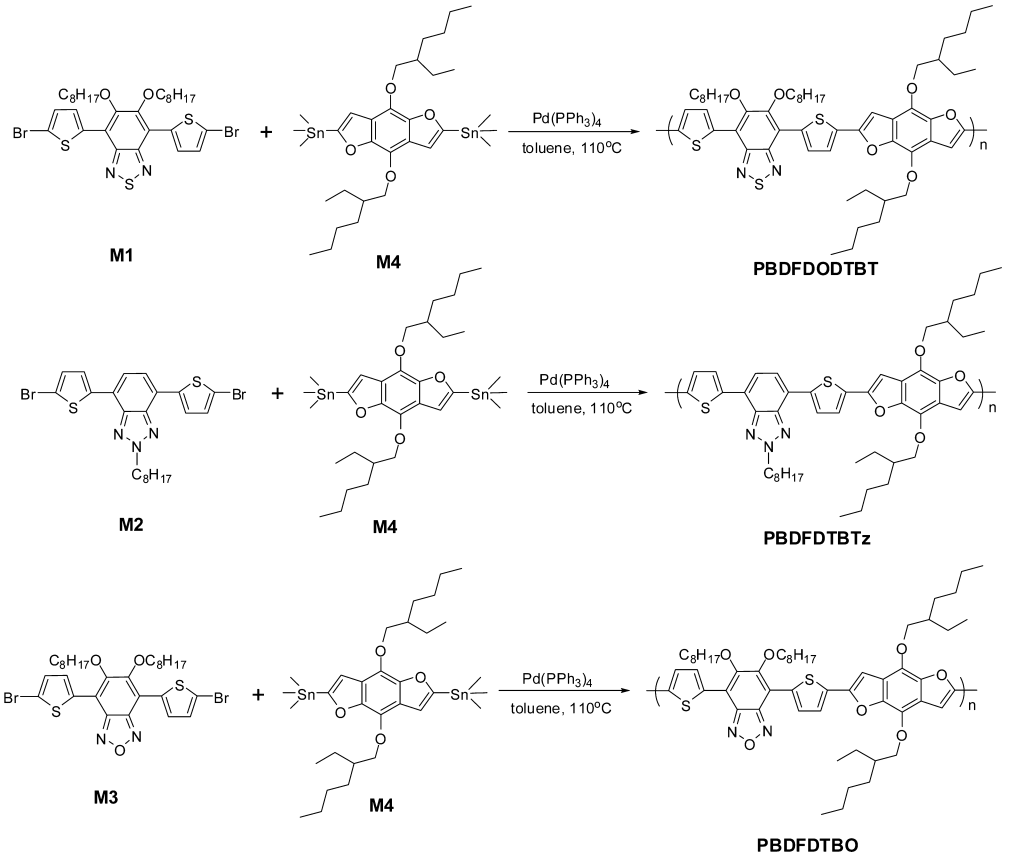

remains still a big challenge to explore D−A copolymers with new donor or acceptor structures to gain further understanding of the structure−property relationships and improve the performance. In search of new donor building block for constructing high performance D−A photovoltaic polymers, a new donor unit—benzo[1,2-*b*:4,5-*b*′]difuran (BDF)—caught our eye. From the reported works, little attention was paid to BDF-based copolymers. To be fact, BDF has a similar fused aromatic structure with BDT using furan ring replacing thiophene unit. Because oxygen atom has less diameter than that of sulfur atom, promoted stacking and well coplanarity conjugated structure can be formed, which is desirable for higher charge mobility and smaller energy bandgap for BDF-based copolymers.[17−19] At the same time, deep HOMO level can be obtained due to higher electronegativity of oxygen atom (O, 3.5; S, 2.5), which usually can lead to higher V_{oc} and stability. On the basis of the above considerations, BDF unit probably will be a class of attractive building block for the design of various types of organic semiconductor materials in the near future. BDF-based copolymers probably possess unique and high photovoltaic properties when combined with a suitable acceptor moiety.

In order to develop the family of the BDF-based D−A copolymers and look for the new conjugated polymers for application as donor materials in PSCs. Here, we synthesized three new BDF-based D−A copolymers (Scheme 1), namely **PBDFDODTBT**, **PBDFDTBTz**, and **PBDFDTBO** by Stille coupling polymerization reactions. However, when we just finished our polymers, Hou et al. reported a BDF-based copolymer with a PCE up to 5% after thermal annealing.[20] This interesting work further intrigued us to investigate the opt-electronic properties of our newly synthesized BDF-based copolymers. Herein, three new polymers are well characterized and the properties are investigated in detail. The copolymers are soluble in common organic solvents with excellent film forming properties. Three copolymers exhibit fine-tunable absorption, energy level, mobilities and morphology, therefore, different photovoltaic properties are obtained. **PBDFDODTBT**: $PC_{71}BM$ (1:2, w/w) blend showed a very high mobility up to 6.7×10^{-2} $cm^2 \cdot V^{-1} \cdot s^{-1}$. The PSCs based on **PBDFDODTBT** as the donor and $PC_{71}BM$ as the acceptor indicated a high PCE of 4.5%. Compared to the corresponding BDT based copolymers, BDF-based polymers demonstrated 1 order of magnitude higher hole mobilities and higher or comparable photovoltaic properties.[21] This work provides a deeper understanding of the structure−property relationships of new BDF-based D−A copolymers. The investigations indicate that BDF probably would be a promising electron donating building block for efficient PSCs.

EXPERIMENTAL SECTION

Materials. Furan-3-carboxylic acid, *n*-BuLi, $Pd(PPh_3)_4$ and Sn-$(CH_3)_3Cl$ were obtained from Acros Organics, and they were used as received. Toluene was dried over P_2O_5 and freshly distilled prior to use. Other reagents and solvents were purchased commercially as ACS-grade quality and used without further purification. 4,7-Di(5-bromothiophen-2-yl)-5,6-dioctyloxybenzo[*c*][1,2,5]thiadiazole (**M1**),[21,22] 2-octyl-4,7-di(5-bromothiophen-2-yl)-2*H*-benzo[*d*][1,2,3]-triazole (**M2**)[23] and 4,7-di(5-bromothien-2-yl)-5,6-dioctyloxybenzo-[*c*][1,2,5]oxadiazole (**M3**)[21,22] were prepared according to the reported procedures. 2,6-Bis(trimethyltin)-4,8-bis(2-ethylhexyloxy)-benzo[1,2-*b*;3,4-*b*′]difuran (**M4**) has been synthesized as we described before.[24]

dx.doi.org/10.1021/ma301053q | *Macromolecules* 2012, 45, 6898−6905

Characterization. ^{1}H NMR spectra was recorded using a Bruker DMX-400 spectrometer, chemical shifts were reported as δ values (ppm) relative to an internal tetramethylsilane (TMS) standard. Number-average (M_n) and weight-average (M_w) molecular weights were measured by gel permeation chromatograph (GPC) method using polystyrene as a standard. TGA was performed on a Perkin-Elmer TGA-7 at a heating rate of 20 K/min under a nitrogen atmosphere. Differential scanning calorimetry (DSC) measurements were performed on a Perkin-Elmer DSCII at a heating or cooling rate of 10 K/min under N_2 . UV−vis absorption spectra were taken using a Hitachi U-3010 UV−vis spectrophotometer. For solid state measurements, polymer solution in chloroform was cast on quartz plates. Optical bandgap was calculated from the onset of the absorption band. Cyclic voltammograms (CV) were recorded on a Zahner IM6e Electrochemical Workstation using platinum disk coated with the polymer film, Pt wire and a Ag/Ag^+ (0.1 M of $AgNO_3$ in acetonitrile) electrode in an anhydrous and argon-saturated solution as working electrode, counter electrode and reference electrode respectively in a 0.1 mol/L tetrabutylammonium hexafluorophosphate (Bu_4NPF_6) acetonitrile solution at a scan rate of 50 mVs^{-1}. The HOMO energy levels were determined from the oxidation onset from the CV spectra, LUMO energy levels were estimated from HOMO levels and optical bandgaps. Electrochemical onsets were determined at the position where the current starts to differ from the baseline. AFM images were obtained using a Veeco's Dimension V atomic force microscopic (AFM) in the tapping mode. Transmission electron microscope (TEM) measurements were performed in a JEM-2100F.

Fabrication of OFET Devices. Thin-film OFETs were fabricated with top-contact configuration. Thermally oxidized (100) silicon wafers (n^{+2} doped) with a SiO_2 thickness of 300 nm were sequentially cleaned with detergent, deionized water, acetone and ethanol in ultrasonic bath. Then hydrophilic treatment of these silicon wafers was performed according to the standard procedure. Briefly, the substrates were soaked in a mixture of deionized water, 25% ammonium hydroxide and 30% H_2O_2 (5:1:1 by volumetric ratio) for 20 min at 80 °C, then rinsed with deionized water and dried with nitrogen flow. Octadecyltrimethoxysilane (OTMOS) was self-assembled on the surface of hydrophilic-treated substrates according to the reported method.[25] Thin polymer films were prepared by spin coating of **PBDFDODTBT** in chlorobenzene onto the OTMOS modified SiO_2/Si substrates at a speed of 3000 rpm (revolutions per minute) for 40 s at room temperature. After annealing at 150 °C under N_2 for half an hour, gold film (50 nm) was deposited on the organic layer to form the drain and source electrodes, for a typical device, the drain-source channel length (L) and width (W) are 80 and 8800 μm, respectively. OFET measurements were performed at room temperature using a Keithley 4200 SCS semiconductor parameter analyzer under ambient conditions.

Fabrication and Characterization of Polymer Solar Cells. The PSCs were fabricated in the configuration of the traditional sandwich structure with an indium tin oxide (ITO) glass positive electrode and a metal negative electrode. Patterned ITO glass with a sheet resistance of 10 Ω/□ was purchased from CSG HOLDING Co. Ltd. (China). The ITO glass was cleaned by sequential ultrasonic treatment in detergent, deionized water, acetone and isopropanol, then treated in an ultraviolet-ozone chamber (Ultraviolet Ozone Cleaner, Jelight Company, USA) for 20 min. The PEDOT:PSS (poly(3,4-ethylene dioxythiophene):poly(styrenesulfonate)) (Baytron P 4083, Germany) was filtered through a 0.45 μm filter and spin coated at 2000 rpm for 60 s on the ITO electrode. Subsequently, the PEDOT: PSS film was baked at 150 °C for 15 min in the air to give a thin film with a thickness of 40 nm. A blend of the polymers and PCBM was dissolved in orth-dichlorobenzene (ODCB), and spin-cast at 3000 rpm for 45 s onto the PEDOT:PSS layer. The substrates were then dried at 70 °C for 15 min. The thickness of the photoactive layer is in the range of 70−100 nm measured by Ambios Technology XP-2 profilometer. A bilayer cathode consisting of Ca (~20 nm) capped with Al (~80 nm) was thermal evaporated under a shadow mask with a base pressure of ca. 10^{-5} Pa. The active area of the PSCs is 4 mm^2. Device characterization was carried out under AM 1.5G irradiation with the intensity of 100 mW/cm^2 (Oriel 67005, 500 W) calibrated by a standard silicon cell. $J-V$ curves were recorded with a Keithley 236 digital source meter.

Synthesis of PBDFDODTBT. **M1** (0.143 g, 0.2 mmol), **M4** (0.148 g, 0.2 mmol), and 10 mL of dry toluene were put into a two-necked flask. The solution was flushed with N_2 for 10 min, then $Pd(PPh_3)_4$ (12 mg) was added into the flask. The solution was flushed with N_2 again for 25 min. The oil bath was heated to 110 °C carefully, and the reactant was stirred for 48 h at this temperature under a N_2 atmosphere. Then the reaction mixture was cooled to room temperature, and the polymer was precipitated by the addition of 100 mL of methanol and filtered through a Soxhlet thimble, which was then subjected to Soxhlet extractions with methanol, hexanes and chloroform. The polymer was recovered as a solid from the chloroform fraction by rotary evaporation. Finally, the blue solid was obtained (0.145 g, yield: 67%). ^{1}H NMR (400 MHz, $CDCl_3$): 8.54 (br, 2H), 7.57−6.75(br, 4H), 4.46−4.22(br, 8H), 2.43−1.17(m, 42H), 1.04−0.71 (m, 18H). Anal. Calcd for $(C_{56}H_{76}N_2O_6S_3)$n (%): C, 69.38; H, 7.9; N, 2.89. Found (%): C, 69.32; H, 8.03; N, 2.75.

Synthesis of PBDFDTBTz. **PBDFDTBTz** was obtained by the similar procedure with the synthesis of **PBDFDODTBT** starting from **M2** (0.111 g, 0.2 mmol) and **M4** (0.148 g, 0.2 mmol). Finally, the deep-red solid was obtained (0.108 g, yield: 59%). ^{1}H NMR (400 MHz, $CDCl_3$): 8.47−6.75 (br, 8H), 4.90−4.00 (br, 6H), 2.43−1.10(m, 30H), 0.96−0.85 (m, 15H). Anal. Calcd for $(C_{48}H_{59}N_3O_4S_2)_n$ (%): C, 71.34; H, 7.61; N, 5.20. Found (%): C, 71.31; H, 7.53; N, 5.39.

Synthesis of PBDFDTBO. **PBDFDTBO** was obtained by the similar procedure with the synthesis of **PBDFDTBT** starting from **M3** (0.14 g, 0.2 mmol) and **M4** (0.148 g, 0.2 mmol). The blue solid was dried under vacuum at 40 °C overnight (0.154 g, yield: 74%). ^{1}H NMR (400 MHz, $CDCl_3$): 8.25−6.52(br, 2H), 4.42(br, 8H), 2.17−0.96(br, 60H). Anal. Calcd for $(C_{56}H_{76}N_2O_7S_2)_n$ (%): C, 70.55; H, 8.04; N, 2.94. Found (%): C, 70.48; H, 8.13; N, 3.09.

RESULTS AND DISCUSSION

Material Synthesis. As shown in Scheme 1, the polymers were synthesized with the ditin derivative (**M4**) in the presence of dibromide (**M1**, **M2** and **M3**) using Stille coupling reactions. The synthesized polymers were purified by continuous extractions with methanol, hexanes and chloroform, and the chloroform fractions were recovered. The chemical structures of the polymers were verified by ^{1}H NMR and elemental analysis. ^{1}H NMR spectra of the polymers are shown in Figure S1, Supporting Information. The polymers exhibited broad resonance and overlapped peaks. The proton signals of the alkyl chain dominated in the region of 0.71−2.43 ppm, the proton signals of $-NCH_2$ or $-OCH_2$ of alkoxyl group appeared at 4.00−4.90 ppm, the proton signals of aromatic group were between 6.50 and 8.50 ppm. The number of aromatic and aliphatic protons estimated from integration of the peaks is basically consistent with the expected repeating unit of the copolymers. Gel permeation chromatography (GPC) results (using polystyrene as the standard and THF as eluent) have shown that the polymers have weight-average molecular weight (M_w) values ranging from 14 kDa to 34 kDa with polydispersities of around 1.2−2.0. The obtained copolymers from chloroform fractions are readily soluble in common organic solvents such as chlorobenzene, tetrahydrofuran and dichlorobenzene, *etc.* Table 1 lists the polymerization results and thermal data of the polymers.

Thermal Stability. Thermal stability of the polymer is important for device fabrication. Figure S2, Supporting Information displays the TGA thermograms of the **PBDFDODTBT**, **PBDFDTBTz** and **PBDFDTBO**. The TGA analysis reveals that, under the protection of an inert

dx.doi.org/10.1021/ma301053q | *Macromolecules* 2012, 45, 6898−6905

Table 1. Polymerization Results and Thermal Data of PBDFDODTBT, PBDFDTBTz, and PBDFDTBO

polymers	M_n (kDa)	M_w (kDa)	PDI	yield (%)	T_d (°C)
PBDFDODTBT	7.0	14	2.0	67	318
PBDFDTBTz	9.6	18	1.9	59	356
PBDFDTBO	27	34	1.2	74	319

atmosphere, the onset points of the weight loss (5%) of **PBDFDODTBT**, **PBDFDTBTz** and **PBDFDTBO** are ca. 318 °C, 348 and 319 °C, respectively. Differential scanning calorimetry (DSC) plots of the polymers are shown in Figure S3, Supporting Information. No appreciable thermal transitions have been investigated during the heating or cooling scans in the temperature range of −20 °C - 280 °C for three copolymers, which indicates the polymers are amorphous due to the introduction of too many long branched side chains. Some very small transitions were observed, which might be originated from the crystallization or the glass transition of the side chains. Relatively high thermal stability of the resulting copolymers prevents the deformation of the copolymer morphology and the degradation of the polymeric active layer under applied electric field. The thermal data of the copolymers are also summarized in Table 1.

Optical Properties. The electronic structure and optical properties of the conjugated polymers can be acquired from UV−vis absorption spectra. The absorption spectra of the synthesized copolymers in solution and thin-film states are shown in Figure 1, and the related optical data are summarized in Table 2. As shown in Figure 1a, three polymers display broad absorption plateau in the dilute $CHCl_3$ solution. The polymers show two absorption bands, the peaks in the long wavelength region locate at 569, 527 and 578 nm, the peaks in the short wavelength region lie at 409, 374, and 404 nm for **PBDFDODTBT**, **PBDFDTBTz**, and **PBDFDTBO**, respectively. The long wavelength absorption is due to strong D−A charge transfer state, which led to the extended absorption. Compared to the solution, three polymers have more red-shifted and broader absorption in the film states as shown in Figure 1b. The broader and better absorption in the solid state is originated from better planarity of the polymer and stronger electronic interaction between the individual polymer chains in the film states. From the onset of the thin film absorptions, we can estimate the optical bandgaps of 1.73, 1.93, and 1.70 eV, respectively for **PBDFDODTBT**, **PBDFDTBTz**, and **PBDFDTBO**. **PBDFDTBTz** blue-shifted ca.60 nm compared to those of the other polymers in the solid films, which is due to decreased internal charge transfer from a relatively weaker electron-withdrawing nature of benzotriazole unit compared to the other two electron accepting unit.[22]

Electrochemical Properties. Cyclic voltammetry was usually performed to determine the HOMO and LUMO energy levels of conjugated polymers. The onset oxidation and reduction potentials obtained from the cyclic voltammograms correspond to the HOMO and LUMO energy levels, respectively. Therefore, we investigated the electrochemical properties of **PBDFDODTBT**, **PBDFDTBTz**, and **PBDFDTBO** by cyclic voltammetry. Figure 2 shows the cyclic voltammograms of **PBDFDODTBT**, **PBDFDTBTz**, and **PBDFDTBO** films on Pt electrode with 0.1 mol/L tetrabutylammonium hexafluorophosphate (Bu_4NPF_6)/acetonitrile (CH_3CN) as the electrolyte at a scan rate of 50 mV·s^{-1} using Ag/Ag$^+$ as the reference electrode. The related electrochemical data are summarized in Table 2. **PBDFDODTBT**, **PBDFDTBTz**, and **PBDFDTBO** exhibit reversible or quasi-reversible oxidation processes. We calculated the HOMO and LUMO energy levels of the polymers according to the equations:[26] HOMO = −e(E_{on}^{ox} + 4.71) (eV). In a positive potential region, the onset oxidation potentials of **PBDFDODTBT**, **PBDFDTBTz**, and **PBDFDTBO** are 0.41, 0.31, and 0.48 eV vs Ag/Ag$^+$, respectively. The corresponding HOMO levels of **PBDFDODTBT**, **PBDFDTBTz**, and **PBDFDTBO** are −5.12, −5.02, and −5.19 eV, respectively. The deep HOMO level of the **PBDFDTBO** is desirable for a higher open circuit voltage of the PSCs. We obtained E_{LUMO} from the E_g^{opt} and E_{HOMO}.[27] The E_{LUMO} values of **PBDFDODTBT**, **PBDFDTBTz**, and **PBDFDTBO** are −3.38, −3.06, and −3.49 eV, respectively (see Figure 3). The LUMO energy level of the polymers is positioned over 0.30 eV than that of $PC_{71}BM$ (3.9 eV, measured under the same condition), which offers enough driving force for charge separation and transfer.[28]

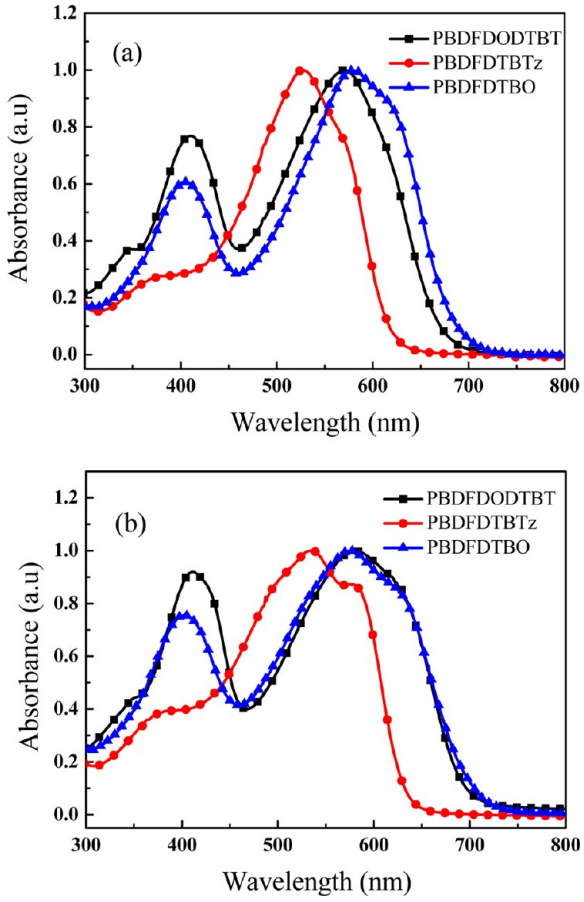

Figure 1. UV−vis absorption spectra of **PBDFDODTBT**, **PBDFDTBTz**, and **PBDFDTBO**: (a) solutions in dilute $CHCl_3$ and (b) films on quartz cast from $CHCl_3$ solution.

Hole Mobility. Besides the absorption and energy levels, hole mobility is another important factor for photovoltaic applications. We measured the hole mobilities of **PBDFDODTBT**, **PBDFDTBTz**, and **PBDFDTBO** blended with $PC_{71}BM$ by SCLC method which is based on the Poole−Frenkel law[29] with a device structure of ITO/PEDOT:PSS/polymers: $PC_{71}BM$ (1:2, w/w) /Au. SCLC is described by

dx.doi.org/10.1021/ma301053q | Macromolecules 2012, 45, 6898−6905

Table 2. Optical and Electrochemical Properties of PBDFDODTBT, PBDFDTBTz, and PBDFDTBO

	absorption spectra				cyclic voltammetry	
	solution[a]	film[b]			*p*-doping	
polymers	λ_{max} (nm)	λ_{max} (nm)	λ_{onset} (nm)	E_g^{optic} (eV)	E_{on}^{ox}/HOMO[d] (V)/(eV)	LUMO[e] (eV)
PBDFDODTBT	569	583	709	1.73	0.40/−5.11	−3.38
PBDFDTBTz	527	536	642	1.93	0.28/−4.99	−3.06
PBDFDTBO	578	580	717	1.70	0.48/−5.19	−3.49

[a]Measured in chloroform solution. [b]Cast from chloroform solution. [c]Bandgap estimated from the onset wavelength of the optical absorption. [d]HOMO = −e(E_{on}^{ox} + 4.71) (eV). [e]LUMO = E_g^{opt} + HOMO.

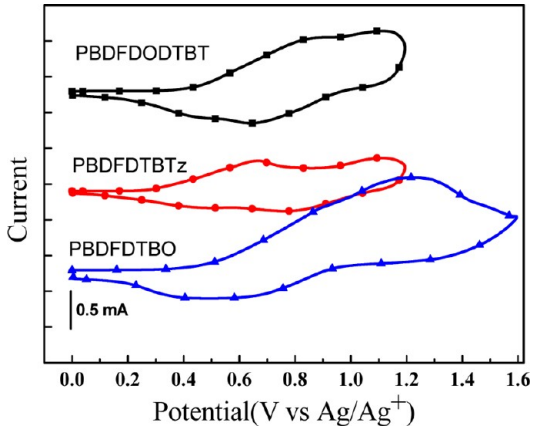

Figure 2. Cyclic voltammograms of **PBDFDODTBT**, **PBDFDTBTz**, and **PBDFDTBO** films cast on platinum wire in 0.1 M Bu_4NPF_6 /CH_3CN solution at a scan rate of 50 mV·s^{-1}.

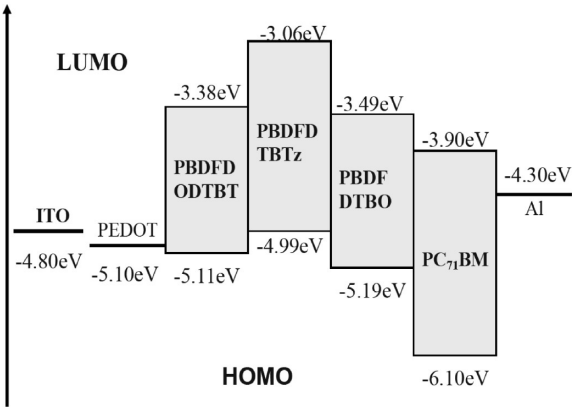

Figure 3. Schematic energy level diagrams of **PBDFDODTBT**, **PBDFDTBTz**, and **PBDFDTBO**.

$$J_{SCLC} = \frac{9}{8}\varepsilon_0\varepsilon_r\mu_0\frac{(V - V_{bi})^2}{d^3}\exp\left[0.89\gamma\sqrt{\frac{V - V_{bi}}{d}}\right] \quad (1)$$

The results are plotted as $\ln(Jd^3/V^2)$ vs $(V/d)^{0.5}$, as shown in Figure 4. Here, J stands for current density, d is the thickness of the device, and $V = V_{appl} - V_{bi}$, where V_{appl} is the applied potential and V_{bi} is the built-in potential. According to eq 1, the average hole mobilities of the blends of **PBDFDODTBT**, **PBDFDTBTz**, and **PBDFDTBO** and $PC_{71}BM$ are 6.72×10^{-2}, 3.69×10^{-3}, and 2.25×10^{-4} cm^2·V^{-1}·s^{-1}, respectively. The hole mobility of **PBDFDODTBT** was much higher than that of **PBDFDTBTz** and **PBDFDTBO** under the same conditions, presumably because of the larger planar structure and closely $\pi-\pi$ stacking of **PBDFDODTBT**, which is beneficial for obtaining higher mobility. As for hole mobility, BDF-based

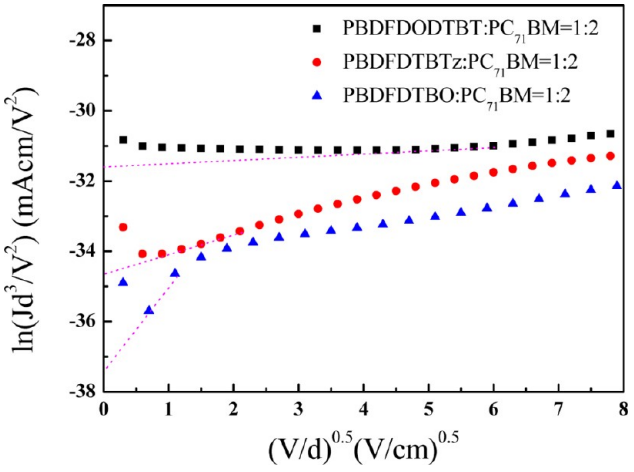

Figure 4. $\ln(Jd^3/V^2)$ vs $(V/d)^{0.5}$ plots of the blends of **PBDFDODTBT**, **PBDFDTBTz**, **PBDFDTBO**, and $PC_{71}BM$ for measurement of the hole mobilities by SCLC method.

copolymers is 1 order of magnitude higher than those of corresponding BDT-based copolymers although of their similar optical bandgaps and energy levels.[21,22] To further investigate the hole mobility, we measured the field effect transistors (FETs) of **PBDFDODTBT**, FET hole mobility of **PBDFDODTBT** is 2×10^{-3} cm^2·V^{-1}·s^{-1} (Figure S4, Supporting Information), which is lower than that from SCLC model. The reason might be from the unoptimized FET device fabrications and different mechanisms from PSCs and FETs. In one word, **PBDFDODTBT** demonstrated a surprisingly high hole mobility among the polymeric photovoltaic materials.[30,31]

Photovoltaic Properties. In order to investigate the potential applications of the three copolymers in solar cells, the bulk heterojunction PSCs were fabricated with a device structure of ITO/PEDOT:PSS/polymers:PCBM/Ca/Al. Photovoltaic devices were tested under simulated 100 mW·cm^{-2}, AM 1.5G illumination. Figure S5 (Supporting Information) shows the current density versus voltage ($J-V$) curves of the device and the detailed device results are summarized in Table S1, Supporting Information. The blends of **PBDFDODTBT** or **PBDFDTBTz** and $PC_{61}BM$ at different weight ratios of 1:1, 1:1.5, 1:2, 1:3, respectively were used to optimize the device performances and their $J-V$ curves are shown in Figure S5, Supporting Information. **PBDFDODTBT** demonstrated much better photovoltaic performance over **PBDFDTBTz**. When **PBDFDODTBT** and $PC_{61}BM$ in weight ratio of 1:2, a best PCE of 3.1% was obtained with a V_{oc} of 0.71 V, J_{sc} of 7.17 mA/cm^2, and FF of 0.60, respectively. In order to achieve a better PCE of the devices, we replaced $PC_{61}BM$ using $PC_{71}BM$ to improve the J_{sc} of the devices because $PC_{71}BM$ has better

dx.doi.org/10.1021/ma301053q | Macromolecules 2012, 45, 6898−6905

absorption than that of $PC_{61}BM$ with similar energy level. As shown in Figure S2, Supporting Information, compared with $PC_{61}BM$ as acceptor, **PBDFDODTBT** and $PC_{71}BM$ in weight ratios of 1:1.5, 1:2, respectively, in all cases, PCEs of the devices above 4.0% were obtained. For the three copolymers, the best ratio of polymer:PCBM is 1:2. The typical *J*−*V* curves are demonstrated in Figure 5 and the corresponding photovoltaic

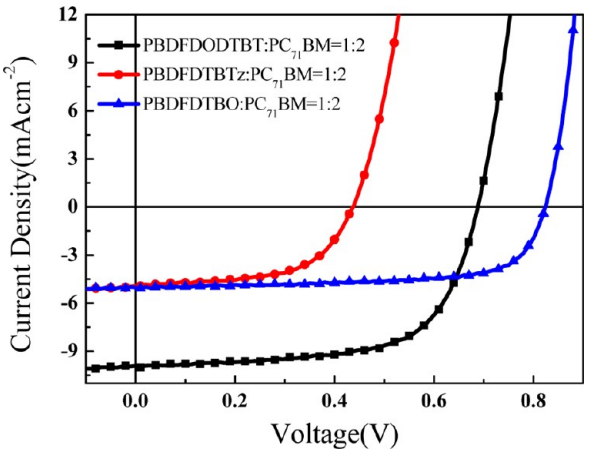

Figure 5. Typical *J*−*V* curves of the polymer solar cells based on polymers:$PC_{71}BM$ with the ratio of 1:2 in ODCB.

Table 3. Photovoltaic Properties of PSCs Based on Polymers:$PC_{71}BM$ (1:2)

active layer	V_{oc} (V)	J_{sc} (mA cm^{-2})	FF (%)	PCE (%)
PBDFDODTBT:$PC_{71}BM$=1:2	0.69	9.87	65.3	4.45
PBDFDTBTz:$PC_{71}BM$=1:2	0.44	4.92	57.5	1.24
PBDFDTBO:$PC_{71}BM$=1:2	0.82	5.04	70.0	2.88

data are listed in Table 3. With a weight ratio of **PBDFDODTBT** to $PC_{71}BM$ of 1:2, a high PCE of 4.5% with a V_{oc} of 0.69 V, a J_{sc} of 9.87 mA/cm^2 and a FF of 0.65 was obtained. For all the polymer based photovoltaic devices, compared with the **PBDFDTBTz** and **PBDFDTBO**, **PBDFDODTBT** obtained a relatively higher PCE, because **PBDFDODTBT** possessed better absorption and higher hole mobility than **PBDFDTBTz.** For **PBDFDTBO,** although of its similar broad absorption, deeper HOMO level compared to **PBDFDODTBT,** however, in the same conditions, it just got the PCE up to 2.88%, which is far lower than that **PBDFDODTBT** (PCE: 4.5%), probably due to 2 orders of magnitude lower in the hole mobilities. **PBDFDTBO** shows the high V_{oc} of 0.82 V due to deep HOMO level. **PBDFDTBTz** has the lowest efficiency of 1.24% among the three copolymers, mainly due to very low V_{oc} of ca.0.44 V from high HOMO level and relatively broad bandgap of 1.93 eV, **PBDFDTBTz** exhibited the similar J_{sc} with **PBDFDTBO**, which may be from the compromise of the hole mobility and absorption of the both copolymers. The three copolymers demonstrated high FF above 0.55, which indicates that the devices have relatively balanced charge transport and low serial resistance in the PSC devices. The accuracy of the photovoltaic measurements can be confirmed by the external quantum efficiency (*EQE*) of the devices. Figure 6 shows the *EQE* plots of the PSC devices

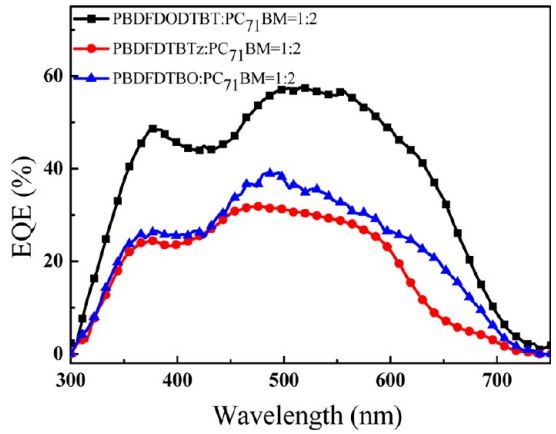

Figure 6. *EQE* curves of the PSCs based on polymers:$PC_{71}BM$ (1:2) in ODCB.

fabricated under the same conditions as those for the *J*−*V* measurements with polymers: $PC_{71}BM$ (1:2). The higher values of *EQE* for the PSC based on **PBDFDODTBT** are consistent with the higher J_{sc} measured in the solar cells. The J_{sc} values obtained from integrating the *EQE* data with the AM 1.5G reference spectrum and from *J*−*V* measurements are very close. The *EQE* results indicate that the photovoltaic results are reliable. The *EQE* values above 40% from 350 to 630 nm of **PBDFDODTBT** led to high J_{sc} close to ca. 10 mA cm^{-2}. The maximum *EQE* plateau reached 57% from 500 to 600 nm. It seems that the higher J_{sc} values of the PSC devices based on the **PBDFDODTBT** might be ascribed to the highest hole mobility and broad absorption.

Morphology. Besides absorption, energy levels and charge mobility, the morphology of the photoactive layer is very critical for PSCs. To better explain different photovoltaic properties and determine if the devices were fully optimized, we investigated the morphologies of the three polymers and $PC_{71}BM$ blends spin-coated from their *o*-dichlorobenzene (ODCB) solution by using tapping-mode atomic-force microscopy (AFM) and transmission electron microscopy (TEM). Figure 7 shows the height and phase images of polymers: $PC_{71}BM$ (1:2, w/w) films. From the height image (Figure 7a,b,c), the root-mean-square (rms) surface roughness values of the blend films for **PBDFDODTBT**, **PBDFDTBTz**, and **PBDFDTBO** are 3.30, 2.91, and 0.77 nm, respectively. Relatively rougher surface with some aggregations were observed from Figure 7, parts a and b, which may be due to close chain packing and crystallization in aggregation form resulting in higher hole mobilities of **PBDFDODTBT** and **PBDFDTBTz** blend with PCBM.[32] From the phase images of the copolymers, **PBDFDODTBT** and **PBDFDTBTz** showed nanoscale bicontinuous phase separation morphology, **PBDFDODTBO** showed very smooth surface without distinct phase separation between the polymer and $PC_{71}BM$. The formation of an interpenetrating bicontinuous network between polymer donor and PCBM with an ideal domain size of 10−20 nm is important for charge generation and transportation.[33] For bulk heterojunction polymer solar cells, nanoscale phase separation is a practical way to form bicontinuous donor−acceptor network.[34] Figure 7 (inset) shows TEM images of polymer/$PC_{71}BM$ blend films prepared using the same conditions as those for the formation of the solar cell active layers. The dark regions were PCBM-rich domains, while bright regions were polymers-rich distributions. The connectivity is

dx.doi.org/10.1021/ma301053q | *Macromolecules* 2012, 45, 6898−6905

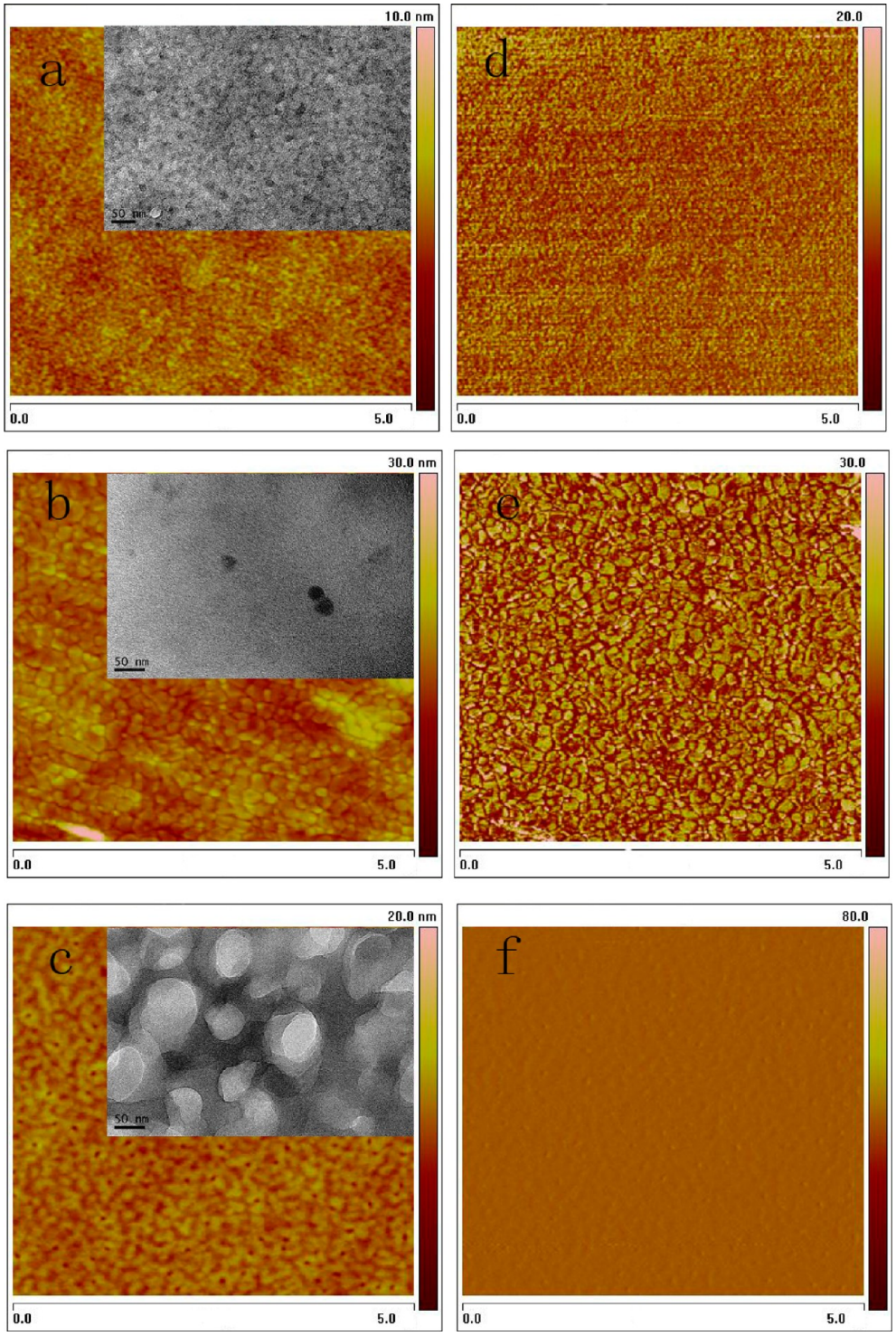

Figure 7. AFM images (5 × 5 μm^2) and TEM images (inset) of polymers:$PC_{71}BM$ (1:2, w/w) blend films spin coated from ODCB: (a and d) **PBDFDODTBT** height image and phase image; (b and e) **PBDFDTBTz** height image and phase image; (c and f) **PBDFDTBO** height image and phase image. TEM scan bar=50 nm.

sensitive to the structures of the polymers. From Figure 7b (inset) to Figure 7a (inset), the fine and nanoscale phase separation can be seen more clearly, **PBDFDODTBT** blend nanostructure is most pronounced among the three polymer blend, implying that long and good connected pathways have been formed, which to some extent explains the better performance of **PBDFDODTBT** based solar cells. However, TEM image of **PBDFDTBO** blend film clearly show polymer spherical domains in some areas with sizes larger than typical exciton diffusion lengths (ca.10 nm), indicating large scale phase separation and no bicontinuous networks, photogenerated excitons will mainly recombine before reaching the interfaces of the donor and acceptor, resulting in poor exciton separation efficiency and low current density. From the above investigations, it is firmly believed that the photovoltaic performance of this type of copolymers can be further

dx.doi.org/10.1021/ma301053q | *Macromolecules* 2012, 45, 6898−6905

improved by the optimization of film morphology and device fabrication conditions.

CONCLUSIONS

In summary, we have designed and synthesized three new benzo[1,2-*b*:4,5-*b*′]difuran containing D−A copolymers. They have been well characterized by ^{1}H NMR, TGA, DSC, UV−vis absorption and cyclic voltammetry. The relationship between the structures and properties was investigated in detail. A high mobility of 6.7×10^{-2} $cm^2 \cdot V^{-1} \cdot s^{-1}$ was obtained from the **PBDFDODTBT** and $PC_{71}BM$ blend by SCLC model. A PCE of 4.5% from **PBDFDODTBT** based polymer solar cells with V_{oc} = 0.69 V, J_{sc} = 9.87 mA/cm^2 and FF = 65.3% was recorded without any device modifications. Those results indicate that **PBDFDODTBT** is a promising candidate for high-efficiency polymer solar cells and benzo[1,2-*b*:4,5-*b*′]difuran unit may be an excellent electron donating building block for organic electronic materials.

ASSOCIATED CONTENT

Supporting Information

^{1}H NMR spectra, TGA and DSC curves, field transistor behaviors, and *J*−*V* curves, with the photovoltaic data summarized in Table S1. This material is available free of charge via the Internet at http://pubs.acs.org.

AUTHOR INFORMATION

Corresponding Author

*E-mail: yingpingzou@csu.edu.cn (Y.Z.); yuehui@csu.edu.cn (Y.H.); liyf@iccas.ac.cn (Y.L.).

Notes

The authors declare no competing financial interest.

ACKNOWLEDGMENTS

This work was supported by the NSFC (Nos. 51173206, 21161160443), the National High Technology Research and Development Program (No. 2011AA050523), the Natural Science Foundation of Hunan Province, China (No. 11JJ4010), China Postdoctoral Science Foundation (No. 20110490150), and the Fundamental Research Funds for the Central Universities (No. 2010QZZD0112).

REFERENCES

(1) Cao, Y.; Parker, I. D.; Yu, G.; Zhang, C.; Heeger, A. J. *Nature* **1999**, *397*, 414.
(2) Grimsdale, A. C.; Chan, K. L.; Martin, R. E.; Jokisz, P. G.; Holmes, A. B. *Chem. Rev.* **2009**, *109*, 897.
(3) Li, Y. F. *Acc. Chem. Res.* **2012**, *45*, 723.
(4) Yu, G.; Gao, J.; Hummelen, J. C.; Wudl, F.; Heeger, A. J. *Science* **1995**, *3*, 270.
(5) Zou, Y. P.; Gendron, D.; Badrou-Aïch, R.; Najari, A.; Ye, T.; Leclerc, M. *Macromolecules* **2009**, *42*, 2891.
(6) Zhou, E. J.; Nakamura, M.; Nishizawa, T.; Zhang, Y.; Wei, Q.; Tajima, K.; Yang, C. H.; Hashimoto, K. *Macromolecules* **2008**, *41*, 8302.
(7) Zhang, Y.; Zou, J. Y.; Yip, H. L.; Chen, K. S.; Zeigler, D. F.; Sun, Y.; Jen, A. K. Y. *Chem. Mater.* **2011**, *23*, 2289.
(8) Wang, E. G.; Hou, L. T.; Wang, Z. Q.; Hellstrom, S.; Zhang, F. L.; Inganas, O.; Andersson, M. R. *Adv. Mater.* **2010**, *22*, 5240.
(9) He, Z. C.; Zhang, C.; Xu, X. F.; Zhang, L. J.; Huang, L.; Chen, J. W.; Wu, H. B.; Cao, Y. *Adv. Mater.* **2011**, *23*, 3086.
(10) Liu, B.; Wu, W. P.; Peng, B.; Liu, Y. Q.; He, Y. H.; Pan, C. Y.; Zou, Y. P. *Polym. Chem.* **2010**, *1*, 678.
(11) Cheng, Y. J.; Yang, S. H.; Hsu, C. S. *Chem. Rev.* **2009**, *109*, 5868.
(12) Li, Y. F.; Zou, Y. P. *Adv. Mater.* **2008**, *20*, 2952.
(13) Hou, J. H.; Chen, H. Y.; Zhang, S. Q.; Li, G.; Yang, Y. *J. Am. Chem. Soc.* **2008**, *130*, 16144.
(14) Wang, M.; Li, C. H.; Lv, A. F.; Wang, Z. H.; Bo, Z. S. *Macromolecules* **2012**, *45*, 3017.
(15) He, Z. C.; Zhong, C. M.; Huang, X.; Wong, W. Y.; Wu, H. B.; Chen, L. W.; Su, S. J.; Cao, Y. *Adv. Mater.* **2011**, *23*, 4626.
(16) Zou, Y. P.; Najari, A.; Berrouard, P.; Beaupré, S.; Aich, R.; Tao, Y.; Leclerc, M. *J. Am. Chem. Soc.* **2010**, *132*, 5330.
(17) Bunz, H. *Angew. Chem., Int. Ed.* **2010**, *49*, 5037.
(18) Tsuji, H.; Mitsui, C.; Ilies, L.; Sato, Y.; Nakamura., E. *J. Am. Chem. Soc.* **2007**, *129*, 11902.
(19) Tsuji, H.; Mitsui, C.; Sato, Y.; Nakamura., E. *Adv. Mater.* **2009**, *21*, 3776.
(20) Huo, L. J.; Huang, Y.; Fan, B.; Guo, X.; Jing, Y.; Zhang, M. J.; Li, Y. F.; Hou., J. H. *Chem. Commun.* **2012**, *48*, 3318.
(21) Ding, P.; Zhong, C. M.; Zou, Y. P.; Pan, C. Y.; Wu, H. B.; Cao, Y. *J. Phys. Chem. C.* **2011**, *115*, 16211.
(22) Bouffard, J.; Swager, T. M. *Macromolecules* **2008**, *41*, 5559.
(23) Zhang, Z. H.; Peng, B.; Liu, B.; Pan, C. Y.; Li, Y. F.; He, Y. H.; Zhou, K. C.; Zou, Y. P. *Polym. Chem.* **2010**, *1*, 1441.
(24) Chen, X. W.; Liu, B.; Zou, Y. P.; Xu, X. J.; Xiao, L.; Guo, X. P.; He, Y. H.; Li, Y. F. *J. Mater. Chem.* **2012**, *22*, 17724.
(25) Ito, Y.; Virkar, A. A.; Mannsfeld, S.; Oh, J. H.; Toney, M.; Locklin, J.; Bao, Z. *J. Am. Chem. Soc.* **2009**, *131*, 9396.
(26) Sun, Q. J.; Wang, H. Q.; Yang, C. H.; Li, Y. F. *J. Mater. Chem.* **2003**, *13*, 800.
(27) Lee, W. H.; Son, S. K.; Kim, K.; Lee, S. K.; Shin, W. S.; Moon, S.; Kang, I. N. *Macromolecules* **2012**, *45*, 1303.
(28) Dennler, G.; Scharber, M.; Ameri, T.; Denk, P.; Forberich, K.; Waldauf, C.; Brabec, C. *Adv. Mater.* **2008**, *20*, 579.
(29) Pasveer, W.; Cottaar, J.; Tanase, C.; Coehoorn, R.; Bobbert, P.; Blom, P.; Leeuw, D.; Michels, M. *Phys. Rev. Lett.* **2005**, *94*, 206601.
(30) Price, S. C.; Stuart, A. C.; Yang, L. Q.; Zhou, H. X.; You, W. *J. Am. Chem. Soc.* **2011**, *133*, 4625.
(31) Jiang, J. M.; Yang, P. A.; Chen, H. C.; Wei, K. H. *Chem. Commun.* **2011**, *47*, 8877.
(32) Li, W.; Zhou, Y.; Andersson, B. V.; Andersson, L. M.; Thomann, Y.; Veit, C.; Tvingstedt, K.; Qin, R.; Bo, Z.; Inganas, O.; Würfel, U.; Zhang., F. *Org. Electron.* **2011**, *12*, 1544.
(33) Blom, P. W. M.; Mihailetchi, V. D.; Koster, L. J. A.; Markov, D. E. *Adv. Mater.* **2007**, *19*, 1551.
(34) Chen, L. M.; Hong, Z. R.; Li, G.; Yang, Y. *Adv. Mater.* **2009**, *21*, 1434.